Method for Identification of Doppler Noise Levels in Turbulent Flow Measurements Dedicated to Tidal Energy

Jean-Baptiste Richard[#1], Jim Thomson[*2], Brian Polagye[*3], Jochen Bard[#4]

[#]*Fraunhofer Institute for Wind Energy and Energy System Technology IWES, Koenigstor 59, 34119 Kassel, Germany*

[1] Jean-Baptiste.Richard@iwes.fraunhofer.de

[4] Jochen.Bard@iwes.fraunhofer.de

[*]*Northwest National Marine Renewable Energy Center, University of Washington, Seattle, WA 98105, USA*

[2] jthomson@apl.uw.edu

[3] bpolagye@uw.edu

***Abstract*— Acoustic Doppler sensors used for flow measurements at energetic tidal sites present an inherent "Doppler noise" in the measured signal, varying with hardware configuration and flow conditions. At scales comparable to the sensors' sampling frequencies, the corresponding perturbations notably contaminate the signal, and cannot be corrected in the time series.**

At such scales, dynamic phenomena are of particular interest in the process of increasing reliability and effectiveness of tidal turbines, and are mostly addressed in terms of statistics. In the case of inflow speed variations, the bias due to Doppler noise should be taken into account, and can be assessed via manufacturer specifications.

Here, a method is presented that enables a direct estimation of the Doppler noise strength from the measured signal itself. Inspired from polynomial least square regression, it is based on a spectral analysis of the measured signal respect to turbulence theory, under the hypothesis of a white Doppler noise contamination. The subsequent limitations are discussed and illustrated by practical cases.

The values found are generally higher than suggested by manufacturers, but still in the same order of magnitude. The use of the highest sampling frequency available is recommended.

***Keywords*— Acoustic, Doppler, Measurement, Noise, Regression, Sampling, Tidal, Turbulence.**

I. Introduction

Tidal streams represent a great resource for renewable energy, with the fundamental advantage of being highly predictable on the timescales of electricity consumption. In contrast, the behavior of TECs with respect to dynamic, short-term variations of tidal stream is not fully understood yet, which represents an important challenge as fatigue loads cannot be neglected in the design of such structures. Also, suitable instrumentation and techniques for measuring those flow characteristics optimally is not clearly identified yet. As they are already widely accepted as a tool for tidal resource assessment, effort is drawn on improving the possibilities of bottom-mounted Divergent-beam Acoustic Doppler Profilers (DADPs[1]), though they were not initially designed for this purpose [1]-[6].

Such sensors nevertheless present some inherent drawbacks for the purpose of measuring flow dynamics. First of them is the presence of an inherent measurement noise, that have been shown to affect Doppler measurements significantly when it comes to analyzing dynamic effects with DADPs [5], but also to a certain extent with Acoustic Doppler Velocimeters (ADVs) despite their higher accuracy and precision [7].

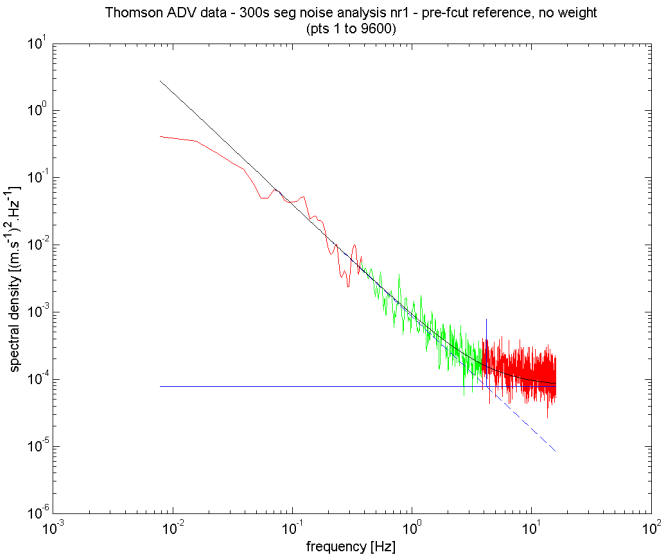

Fig. 1: Example of measured spectra measured with an ADV (red), with proposed analysis performed on the green bandwidth. Mean speed is 1.54 $m.s^{-1}$, estimated noise standard deviation is 3.5 $cm.s^{-1}$.

Estimates of the Doppler noise bias, depending on the configuration of the sensors, are given by manufacturers'

[1]The acronym "ADCP" is often used for naming such sensors, but is a trademark of Teledyne RD Instruments and theoretically refers to their products only. "DADP" is therefore used here generically, as the method applies equally on other products such as the "AWAC" or "Aquadopp Profiler" from Nortek.

documentation and software [8]-[9]. It can also be estimated by averaging the high-frequency end of the signal spectra [10], when the measurement sampling frequency is high enough.

In this paper, a method is presented that enables estimating Doppler noise contamination of the signal, with much lower requirement on the sampling frequency.

The hypothesis and mathematical development are detailed in chapter II. The method is then applied to different datasets: first, single-point high-resolution ADV data is used to assess the robustness of the method in part III.A; the procedure is then run on DADP data, as such sensors have extra capabilities to measure flow speeds across the whole water column. This is presented in part III.B. Conclusions are finally drawn in chapter IV.

It has to be noted that this method can also be used for directly assessing TKE dissipation rate from noise-contaminated measurements, but that is not in the focus of this paper.

II. THEORY

A. Hypothesis and their justification

The hypotheses of the method are based on the one hand on the characteristics of the flow, and on the other hand on the analysis of the acquisition method.

1) Inertial Range and Frozen Turbulence Hypotheses: With speeds of $\mathcal{O}(1\text{m.s}^{-1})$, length scales of $\mathcal{O}(10\text{m})$, density of $\mathcal{O}(1000\text{kg.m}^{-3})$ and kinematic viscosity of $\mathcal{O}(10^{-3}\text{Pa.s})$, tidal flows relevant for energy extraction have Reynolds numbers around 10^7 and are therefore fully turbulent. According to Kolmogorov's theory, in the length scale domain ranging from the integral scale to the Kolmogorov scale and called the inertial range, the Turbulent Kinetic Energy Density (TKED) varies with wavenumber k as

$$TKED(k) = C\varepsilon^{2/3}k^{-5/3}, \quad (1)$$

with C being the Kolmogorov constant and ε being the turbulent kinetic energy dissipation rate.

Furthermore, assuming that the turbulent eddies are advected by a mean flow U, and that the speed fluctuations u respect to this moving frame of reference are small in comparison with U, one can assume through the Frozen Turbulence Hypothesis (FTH) that the frequencies f of phenomena recorded at a fix point of observation are related to the wavenumbers by $f = k/U$. Considering that the TKED is equal to the Power Spectral Density (PSD) S of the velocity fluctuations, one can write that in the inertial range,

$$S(f) = K \times f^{-5/3}, \quad (2)$$

with K being a constant.

In Fig. 1, the low-frequency end of the inertial range can be observed around 0.1 Hz. As summarized by Durgesh et al, it is expected to extend in the high frequencies beyond 10^3 Hz in the flows of interest [10], but in Fig. 1 is obscured by Doppler noise.

2) White Noise, and Relation with the Standard Deviation of Measured Speed:

The dynamic phenomena of interest come out as variations in the measured speed signal. As its values are real, corresponding spectral analysis can be performed as single-sided PSD estimate, whose integral is an estimate of the signal variance. From equation (2), the PSD estimates of the signal should tend to zero with increasing frequencies. For analyses of measured signals, this is not the case because of measurement noise. Such additional measurement fluctuations add variance to the signal:

$$\sigma^2_{measured} = \sigma^2_{physical} + \sigma^2_{noise}. \quad (3)$$

From a spectral point of view, this noise-induced variance is distributed as additional PSD layer over the whole frequency domain. It is commonly accepted (e.g. [11],[12]) that the errors in consecutive acoustic pings are uncorrelated, and therefore that this increase in PSD is statistically independent of the frequency. This can be referred to as "white noise" as a parallel to white light covering all frequencies of the visible light spectra.

As a consequence:

- at high frequencies, the measured spectrum is saturated by noise and converges to the noise PSD, denoted N in this paper, rather than tending to zero. This is clearly illustrated in [10] with the figure hereunder, where B represents the additional noise-related variance:

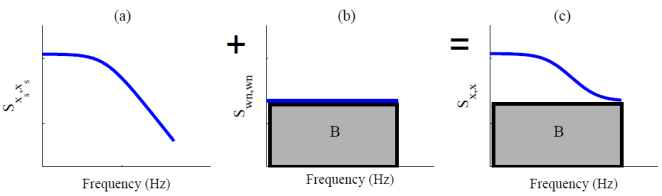

Fig. 2: Schematic showing the effect of white noise contamination in the auto-spectral density function: (a) schematic of auto-spectral density function of clean signal, (b) schematic of auto-spectral density function of white noise, and (c) schematic of auto-spectral density function of clean signal with white noise. Axis are in logarithmic scale. Source: [10].

- The variance of the measured signal is biased by the integral of N over the bandwidth of the spectra.

Also, with:

- the high-end frequency of the spectra equal to half the sampling frequency f_s,
- the low-end frequency of the spectra, depending on the spectral analysis segment duration, being negligible with respect to f_s,

the bias in measured variance due to the noise can be approximated by

$$\sigma^2_{noise} \approx N \times f_s / 2. \quad (4)$$

B. Limitations of the Method Respect to the Hypothesis

1) Beam Separation:

In the case of of DADP data post-processed with standard methods, speed estimates measured at a given elevation z above the sensor are based on acoustic measurements

performed at different reference points of the corresponding horizontal layer. Those points are distant one from another, of a distance called "beam separation" and very similar to *z* for diverging beam angles of 20-25° [6]. One can then define a Beam Separation critical frequency

$$f_{BS} = U / z, \quad (5)$$

corresponding to the time one particle of the ambient flow needs to cover the beam separation. While observing a phenomenon occurring in the flow at a frequency f, in the case where no Doppler noise corruption occurs:

- if $f << f_{BS}$, the manifestations of the phenomena at the different reference acoustic measurement points tend to be the same, hence an expected good fidelity of the measurement.
- If $f >> f_{BS}$, the manifestations of the phenomena at the reference points are not expected to be correlated. The individual measurements are therefore expected to be intrinsically corrupted. Nevertheless, their magnitude is expected to stay proportional to the magnitude of the actual phenomena, via a factor that depends on the slant angle of the acoustic beams. In terms of spectral analysis, the PSD estimate at such frequency is multiplied by the square of this factor. With a logarithmic y-axis graph, this implies a vertical translation of the PSD curve.

In the inertial range, both of those two cases lead to a speed PSD proportional to $f^{5/3}$ as in Eq. (2), which is one base hypothesis here. Nevertheless, in the transition between those two domains, discrepancies are expected. They can affect the regression process while occurring in a part of analysis bandwidth not saturated by noise. The Beam Separation critical frequency is typically in the 0.1-1 Hz domain, given values of *U* and *z* typical for tidal energy sites.

2) Waves:

In addition to the turbulence caused by the tidal flow itself, surface waves, when present, can be an important source of variation of the water speed over time. This is due to the induced orbital speeds, which extend down the water column up to a depth of half the corresponding wavelength. Those fluctuations obey different laws compared to turbulence. In velocity spectra, they lead to a PSD raise in the frequency range of wave-related surface elevation spectra, typically in the 0.1-1Hz domain.

In the case of DADP measurements, a precise assessment of this variation in the PSD requires coupling the precise knowledge of the wave-induced velocity with the intrinsic post-processing of the sensor, directly related to its geometry. This is not covered in the present study.

3) Noise Pattern:

In the low-frequency domain of flow speed measurements, the physical phenomenon largely prevails in the PSD magnitude. As a consequence, there is relatively less knowledge of the noise pattern in this part of the spectra bandwidth than there is for the high-frequency side. One could therefore consider the white noise hypothesis not to be very robust, but the impact of this uncertainty is quite negligible due to the relatively little importance of low-frequency domains while integrating PSDs of same order of magnitude over the whole bandwidth.

C. Least-Square Regression

In order to assess the noise saturation level of such spectra, a method is derived from least-square polynomial regression. It aims at fitting, over a given reference bandwidth, a *S*(*f*) spectrum with a two-parameter curve of equation

$$Y = \left(K \times f^{-5/3} + N\right), \quad (6)$$

with $K = \alpha\varepsilon^{2/3}$ and N being the PSD of the Doppler noise.

Let the spectrum being numerically defined as discrete values S_i at frequencies f_i, for each data point *i* of the reference bandwidth. The differences d_i between the measured spectra and the fitted curve are:

$$d_i = S_i - \left(N + K \times f_i^{-5/3}\right). \quad (7)$$

The least-square procedure fits the curve to the experimental data by minimizing an error *E* defined as the sum of the square of those individual offsets, optionally weighted with coefficients $c_i \geq 0$. With *M* data points taken into consideration in the measured spectra, this sum to be minimized as a function of the parameters *N* and *K* is:

$$E(N,K) = \sum_{i=1}^{M} c_i d_i^{\,2} = \sum_{i=1}^{M} c_i \left[S_i - \left(N + K \times f_i^{-5/3}\right)\right]^2 . \quad (8)$$

As *E* is both continuous and differentiable for *N* and *K*, if a minimum of *E* exists, then the partial derivative of *E* with respect to N and K must be null at this minimum, which can be written as a set of two equations,

$$\left\{ \begin{array}{l} \dfrac{\partial E}{\partial N} = -2\sum_{i=1}^{M} c_i \left[S_i - \left(N + K f_i^{-5/3}\right)\right] = 0 \\ \dfrac{\partial E}{\partial K} = -2\sum_{i=1}^{M} c_i \, f_i^{-5/3} \left[S_i - \left(N + K f_i^{-5/3}\right)\right] = 0 \end{array} \right\}, \quad (9)$$

that is eventually equivalent to the well-defined linear system:

$$\begin{bmatrix} \sum_{i=1}^{M} c_i & \sum_{i=1}^{M} c_i \, f_i^{-5/3} \\ \sum_{i=1}^{M} c_i \, f_i^{-5/3} & \sum_{i=1}^{M} c_i \, f_i^{-10/3} \end{bmatrix} \begin{bmatrix} N \\ K \end{bmatrix} = \begin{bmatrix} \sum_{i=1}^{M} c_i S_i \\ \sum_{i=1}^{M} c_i S_i f_i^{-5/3} \end{bmatrix}, \quad (10)$$

which can be easily solved numerically for *N* and *K*.

Two weighting schemes are investigated in this paper. In a first formulation, all weighting coefficients are set equal. This simplest and neutral approach is not expected to be the most robust, due to the PSDs of the signal varying in orders of magnitude in the domain of interest: relatively small discrepancies from the hypothesis in the PSDs from the low-

frequency side of the reference bandwidth are anticipated to potentially have a significant impact on the final estimates.

Second, as the considered spectra are typically presented in log-log coordinates, a corresponding weighting scheme is implemented, with weighting coefficients intended to account for logarithmic evolution of PSDs on the frequency range and to balance the evolution of density of information with a logarithmic x-axis.

III. Application of the Regression Method on Different Measurement Datasets

Though the main objective is to quantify the noise bias in DADP measurements, the method is first applied on data measured with ADV. This is because those are more precise and have a much higher temporal resolution, and can therefore be used both as reference and for simulating poorer quality measurements of the same phenomena. Subsequent comparisons then provide information on the efficiency and robustness of the method.

A. Application of the method on ADV data for reference considerations, and subsequent analysis

The ADV measurements were recorded during 4 days of February 2011, at a sampling frequency of 32 Hz, in Puget Sound, WA, USA. The hardware used was a 6MHz Nortek ADV. Data collection is described in [5], with data preparation and quality control being documented in [13].

As these data do not come from DADP but from single-point sensor, they are not subject to beam separation consideration discussed in II.B. Also, the measurement was performed in a channel with relatively quiet wave climate, and more than 15 m under the mean free surface, and traces of wave orbital velocity are therefore expected to be negligible. This fidelity of the dataset respect to the method's hypotheses makes it ideal for a first level of testing.

The quantity analyzed here is the measured instantaneous magnitude of the velocity. The signal is treated as 1256 non-overlapping segments of 5 minute duration (i.e., 9600 points per sample at 32 Hz). After removal of the mean and linear components, the PSD estimate of each segment is calculated through Matlab's Pwelch function with default parameters (8 windows, modified by a Hamming filter, each overlapping by 50%). The regression algorithm is then applied to different portions of the obtained spectra.

First, an analysis is performed without weighting using the last two decades of the spectra, that is to say from 0.16 to 16 Hz. This bandwidth extends to the maximum available high frequency for approaching noise saturation, and starts just beyond the integral scale on the low frequency end. The obtained curve fitting and the corresponding values of K and N are therefore reliable and used as reference. Two extreme examples are presented in Fig. 3.

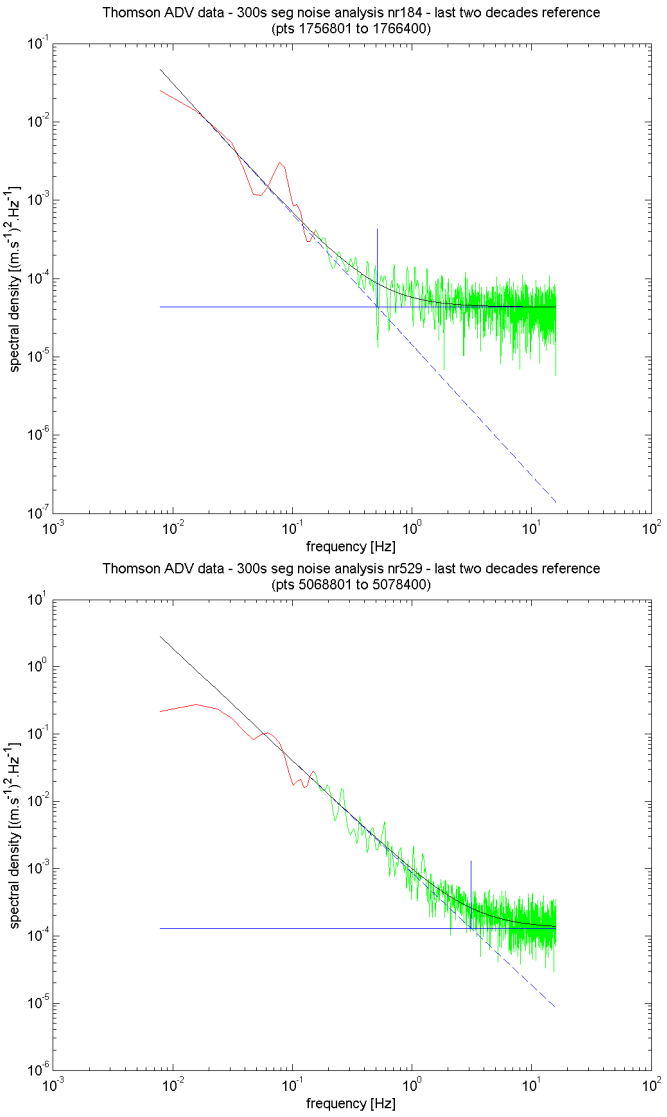

Fig. 3: Example reference fittings for very low (0.17 m.s^{-1}, top) and very high (1.83 m.s^{-1}, bottom) mean speeds. Estimated noise standard deviations are 2.6 and 4.6 cm.s^{-1}, respectively.

At this stage, one can deduct important characteristics of this measurement. First, the estimated noise standard deviation varies with respect to the mean speed, as illustrated in Fig. 4. It clearly appears that this noise bias is increasing with the measured speed. One can also see that, apart from some cases at very low speeds, the computed bias is above the 0.02 m.s^{-1} reference value reported in [5].

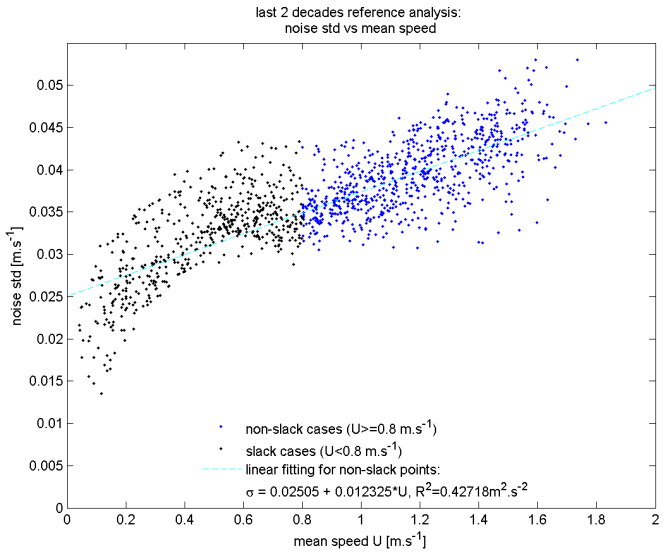

Fig. 4: Noise standard deviations for ADV measurement: references computed with the method applied on the last two decades of the spectra, and plotted against the corresponding mean speed. Linear trend is calculated for non-slack conditions.

The second key figure deducted from this reference fit is the cutting frequency defining the frontier between a low frequency domain where the PSD of the physical speed prevails on the noise, and a high frequency domain where the noise dominates. We denote it f_{cut} in this paper:

$$f_{cut} = \left(\frac{N}{K} \right)^{-3/5} . \qquad (11)$$

It is found varying from 0.2 to 5 Hz, increasing with the mean speed., as can be seen in Fig. 5. This is consistent with an increase in TKE with speed (i.e., increasing signal to noise ratio).

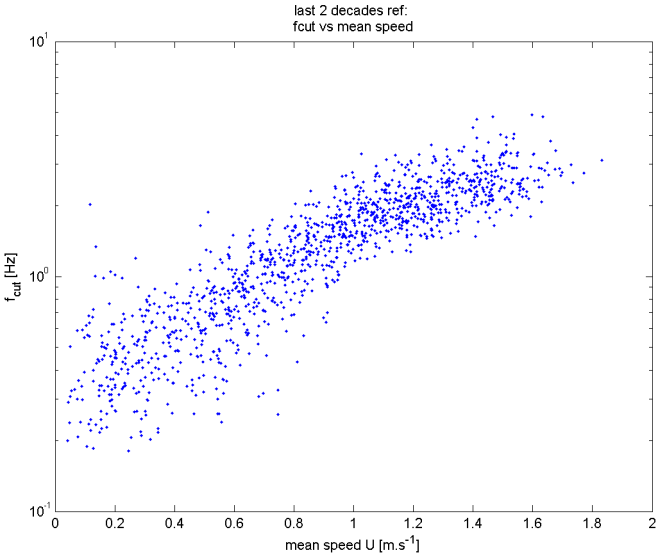

Fig. 5: Cutting frequencies (f_{cut}) for ADV measurements: references plotted against the corresponding mean speeds.

With those characteristics of the high-resolution measurement, the next step is to investigate the robustness of the method by artificially lowering the quality of the data. This is done by reducing the bandwidth used in the analysis: decreasing its upper bound is equivalent to analyzing the same measurement recorded at a lower sampling frequency, provided that this change in sampling frequency only results from a change in ensemble averaging without decimation. In other words, the noise level of the individual acoustic pings is not changed, only the overall quantity of available information is affected by averaging (i.e. loss of high-frequency contents).

Namely, one-decade parts of the spectra are used for the following test analyses. For each segment, 2 test bandwidths are defined based on the reference cutting frequency. The first one is centered on it, that is to say ranges from $\sqrt{0.1} \times f_{cut}$ to $\sqrt{10} \times f_{cut}$, for capturing the transition between target and noise-dominated parts of the spectra. The second one extends only on the low-frequency side of f_{cut}, and therefore contains relatively low noise.

The method is applied on each of the two spectrum extracts, both with and without the weighting scheme described in §II.C. Fig. 6 presents the noise estimates obtained in those 4 cases, compared against the reference noise estimates, for the 1256 segments.

Graph (a) of Fig. 6 shows that with input data reduced to the “transition” bandwidth, the algorithm without weightings gives quite acceptable noise estimates.

For lower frequency bandwidths containing just one side of the transition, the results, illustrated in graph (b), are scattered more widely aside the references. In addition, the model presents robustness limits: for some segments, the regression gives negative estimates for the noise variance. This corresponds graphically to a vertical spectra asymptote instead of an horizontal one.

As can be seen on graph (d), the number of those inconsistencies falls when using the weighting coefficients in the regression: it goes from 125 to 50, corresponding to 10% and 4% of the segments, respectively. The distributions of those errors respect to the mean speed are detailed in Fig. 7. For both approaches, the proportion of errors is greater at low speeds, whether with reference to the total number of errors in the results or respect to the total number of cases for a given mean speed range. This trend is clearer when using the weightings, that also somehow reduce the dispersion of the noise estimates for those low-frequency bandwidths.

Nevertheless, as can be seen in graphs (c) and (d) of Fig. 6, the weightings lead to an underestimation of the noise intensity, at least on average, for both of the two bandwidth types used here.

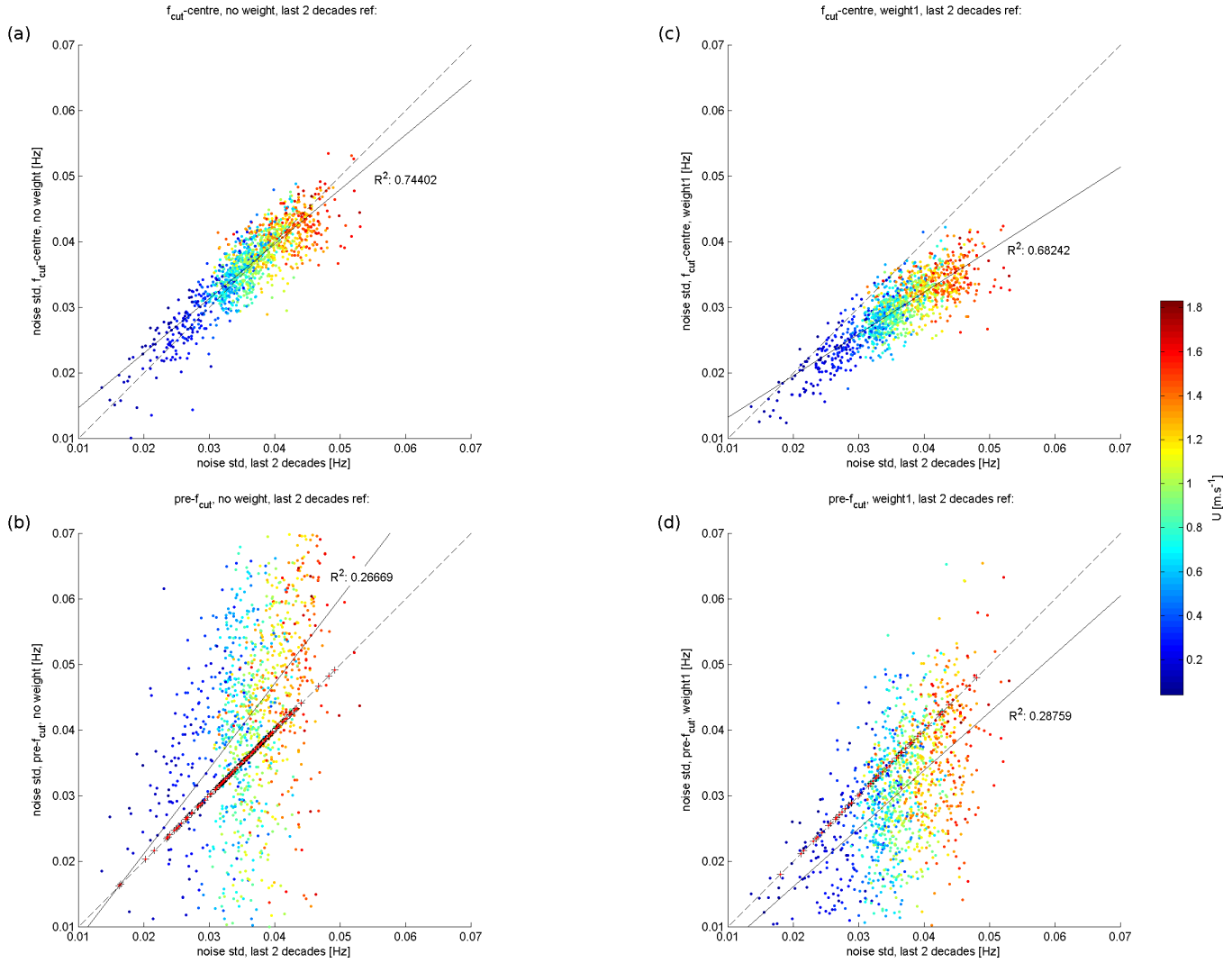

Fig. 6: Comparisons of noise standard deviations: test analyses against reference. Dashed lines mark 1:1 agreement.Solid lines are the linear trends. Left and right plots are for regression without and with weightings, respectively. Top plots correspond to analyses on bandwidth centred on f_{cut}, while bottom plots correspond to pre-f_{cut} bandwidth. Test analyses that gave negative noise variance estimates are indicated by red points on the 1:1 agreement line.

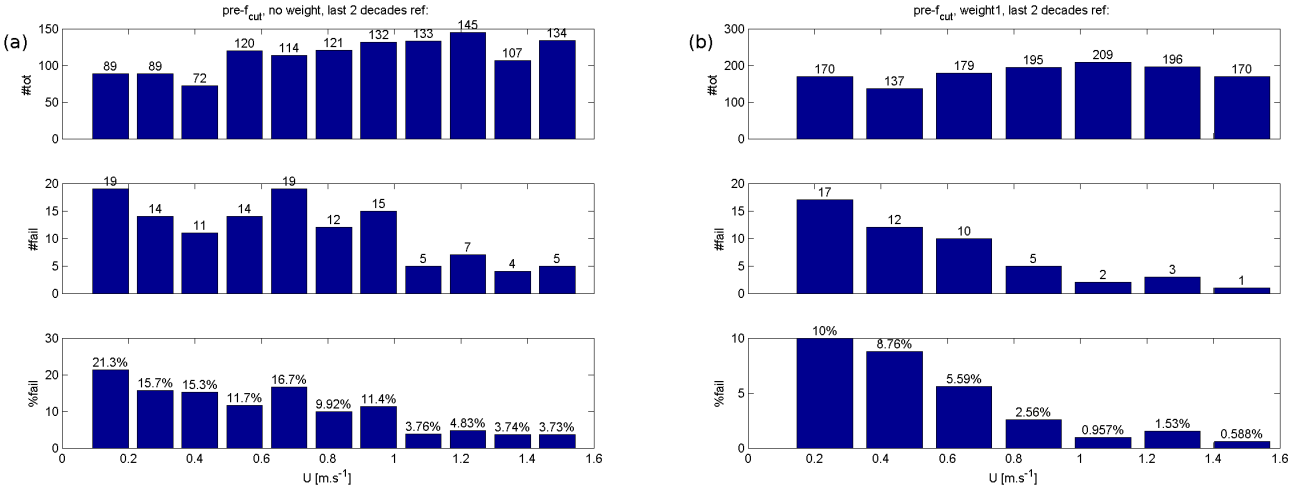

Fig. 7: Distributions of analyses respect to the mean speed for non-weighted (a) and weighted (b) regressions. Top histograms describe the overall distribution of the 1256 segments, middle histograms shows distributions of inconsistent pre-f_{cut} analyses that estimate a negative noise variance, bottom histograms draw which proportion of each top-histogram bar consists of such failed analyses.

B. *Application of the method on DADP data, and subsequent analysis*

After application on the previous dataset, considered ideal for testing the method within its hypothesis, the method is applied on DADP data. One of the particular points here is the beam spread consideration.

This second dataset has been measured at the same place and time with the ADV data analysed in §III.A, and is also described in [5]. It is performed with a 600kHz RDI Workhorse ADCP and the data are recorded in beam coordinate, i.e. before post-processing [8]. The sampling frequency is 2Hz, bin size is 0.5m with the ADV measuring in the horizontal layer of bin 4.

The data is analysed in segments of 10 minute duration, corresponding to 1200 point length. Points discarded by quality control (strength of backscattered signal under threshold) represent between 3 and 3.5% of the signal for bins 1 to 20. They are not replaced by any correction method: only segments of consecutive valid data are analysed, representing 40% of the total measurement time series.

The corresponding spectra being almost saturated by noise, analyses are performed on the last decade without the weighting scheme. Both beam speeds and horizontal velocity magnitude are investigated.

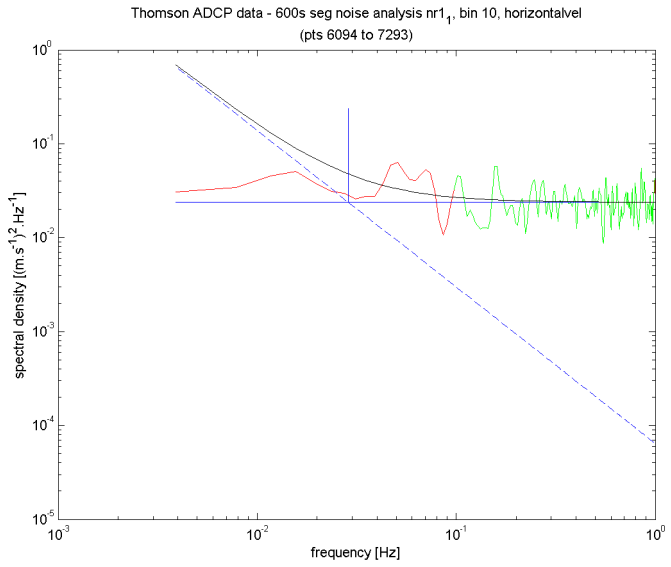

Fig. 8: Example analysis on Thomson's [5] ADCP data. Due to quite high noise level, the elevation of the $f^{5/3}$ slope corresponding to the flow characteristics can hardly be assessed directly, but the noise estimation is assumed to be good. Mean speed is 0.75 m.s^{-1}, noise estimated standard deviation is 0.15 m.s^{-1}, turbulence intensity is 22% without correction and estimated to 7% after noise correction.

As horizontal speed analyses are subject to be altered by the beam separation aliasing effects discussed in §II.B, an indicative equivalent horizontal speed component noise standard deviation is calculated from the beam speed noise standard deviations: assuming the pitch and roll influence are negligible, each horizontal speed component is a linear function of two beam speeds in the form:

$$x = \frac{1}{2\sin(\theta)}(b_1 - b_2), \qquad (12)$$

with θ the beam slant angle [8]. The corresponding variance can be written:

$$\sigma_x^2 = \left(\frac{1}{2\sin(\theta)}\right)^2 \left[(\sigma_{b_1}^2 + \sigma_{b_2}^2) - 2Cov(b_1, b_2)\right]. \qquad (13)$$

Under the previous assumption that a part of it is due to flow dynamics and the other one is due to Doppler noise, and that:

- at given flow conditions, the noise variances of the beam speeds are equal to a value $\sigma_{noise\,beam}$;
- noise in each beam speed is independant from any other quantity, i.e. coviariances between noises of different beams, and covariances between noise and instant speed, are null;

it comes:

$$\sigma_{noise\,x} = \frac{1}{\sqrt{2}\sin(\theta)}\sigma_{noise\,beam}, \qquad (14)$$

independently of what correlations between flow speeds in measured beam velocities could be. In other words, the noise in the inclined beams is projected onto the horizontal plane.

The results of the analyses on bin 20, 10, and 4 are illustrated in Fig. 9, with top-to-bottom order referring to the position of the measurements in the water column.

One of the first things that one can notice is that for a given mean speed and elevation, the noise contamination of the four beam speeds has a very similar intensity.

Also, a discrepancy between horizontal speed magnitude noise and horizontal equivalents based on beam analysis is clear at low speeds, under 0.6 m.s^{-1}. This is because those equivalents refer to the two components of the speed. They have an impact on both magnitude and directionality, the later being not represented here and with increasing importance with decreasing speed.

Appart from that, the horizontal equivalents appear to match the horizontal estimates quite well on the rest of the velocity range. This indicates that beam spread does not perturbate the analyses on horizontal speed in this dataset, and that beam speed analysis could be used to avoid beam spread effects while assessing the noise contamination of horizontal velocity measurement.

The next point of interest is the values found for the standard deviation due to Doppler noise. As reported in [5], the PlanADCP software indicates a reference of 0.156 m s^{-1}. It appears here that the contaminations are slightly higher. They also tend to increases with the mean speed, this being more sentive in the lower part of the water column. The results shown in Fig. 9c are consistent with the value of 0.174 m.s^{-1} found experimentally in [5] by comparison of bin 4 data with ADV data for speeds above 0.8 m.s^{-1}.

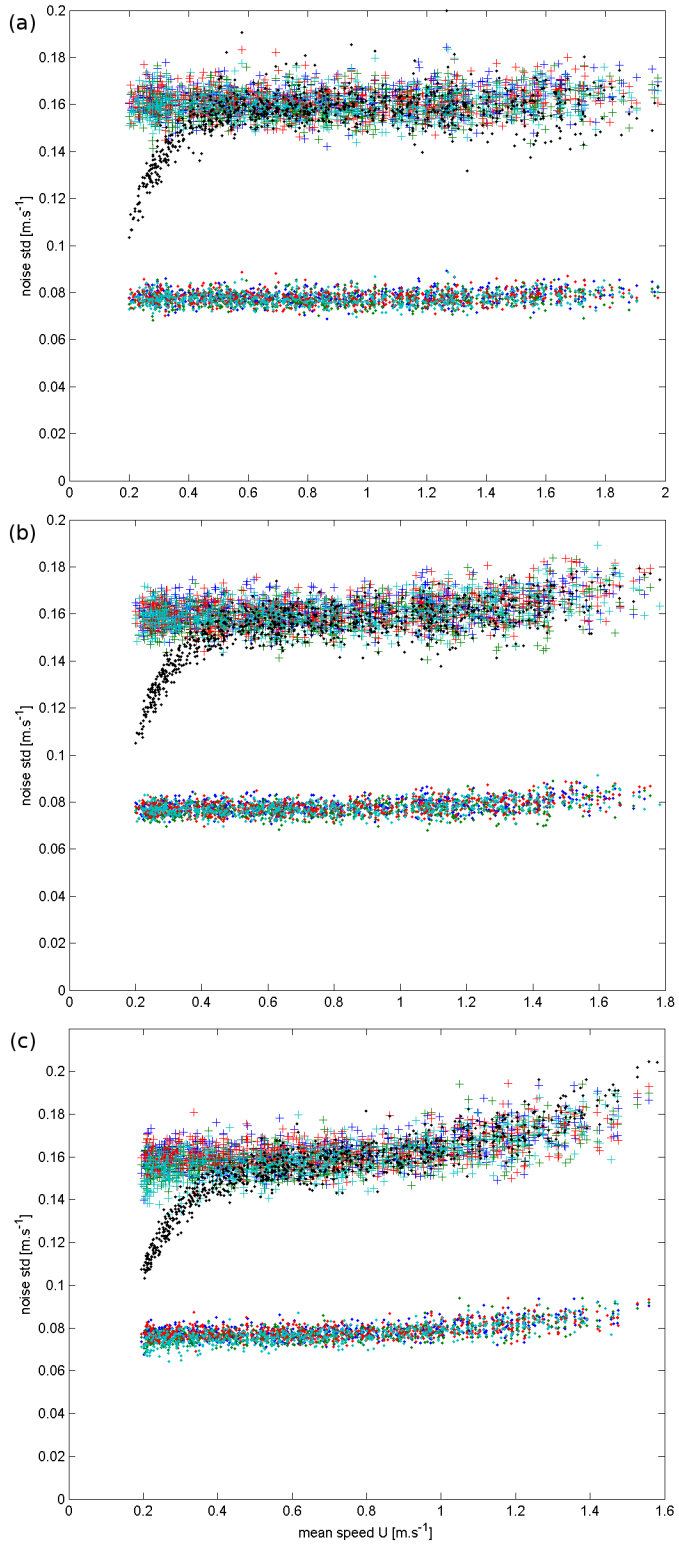

Fig. 9: Noise standard deviations calculated for bins 20 (a), 10 (b), and 4 (c) of Thomson ADCP data, as a function of mean speed. Positions in the water column are 12.65, 7.65, and 4.65 meters over bottom, respectively. Black dots correspond to the noise on horizontal speed magnitude calculated from the PSD of horizontal velocity, coloured dots to noise beam speed signals calculated from the PSD of beam velocities, while coloured crosses are beam speed noise standard deviations scaled to horizontal speed component equivalent.

IV. Conclusions and Future Work

A mathematical method for assessing Doppler noise contamination in tidal flow speed measurement performed with hardware based on acoustic Doppler principle has been described, with its hypothesis and their limitations. Its application on two reference datasets has been presented.

The analyses on ADV data show that, with input signal respecting well the hypothesis, the method is expected to be stable and accurate for sampling frequencies half a decade greater than a cutting frequency where the measurement noise and the fluctuations of the flow speed have the same PSD. With a sampling frequency equal to this cutting frequency, the stability of the model is affected but can be somewhat improved by applying a weighting scheme in the mathematical model.

Further work could determine appropriate time-series treatment to be applied on those estimates, if necessary calculated in parallel with different weighting schemes, that would aim at correcting under- or overestimations, scattering, and missing values. Such treatment should make use of segment overlapping for getting greater density of estimates over time and eventually real-time treatment capabilities.

Analyses on ADCP data provided information on other aspects and perspectives of the method. They show good agreement with a recent study enquiring the same topic by other means, and provided confidence in overcoming beam spread effect if necessary.

Nevertheless, study on other datasets with apparent lower noise contamination (not shown here) demonstrated that waves can have a strong impact on the robustness of the method, as it has been reported to be the case for the variance method [4]. This is believed to be possible to address by appropriate weighting in the regression, filtering out the corresponding frequencies on a bandwidth as small as possible.

This work seeking a better knowledge of limitations inherent to flow measurement sensors for the purpose of the characterisation of tidal flow dynamics is part of the research activities of the MaRINET project. In this framework, the method is planned to be applied on different hardwares, and and different configurations of same hardware, by the end of 2013 [14].

It is also part of an international initiative, so far informal, aiming at a better understanding of the interaction between tidal flow turbulence and tidal turbines. International collaboration is essential to advancing the state of the art in tidal turbulence measurements.

Acknowledgments

The authors would like to thank J. Talbert and A. de Klerk for deployment and recovery engineering of the Puget Sound measurements, and Captain A. Reay-Ellers for the corresponding ship operations.

The main author's research is partially funded by the European Union through the Seventh Framework Programme (FP7) MaRINET project (grant agreement No. 262552).

REFERENCES

[1] A. E. Gargett, "Observing turbulence with a modified acoustic Doppler current profiler", *J. Atmos. Oceanic Technol.*, vol. 11, no. 6, pp. 1592-1610, Dec. 1994.

[2] M. T. Stacey, S. G. Monismith, J. R. Burau, "*Measurements of Reynolds stress profiles in unstratified tidal flow*", J. Geophys. Res.: Oceans, vol 104, no. C5, pp 10933-10949, May 1999.

[3] Y. Lu, R. G. Lueck, "Using a Broadband ADCP in a Tidal Channel. Part II: Turbulence", *J. Atmos. Oceanic Technol.*, vol. 16, no. 11, pp. 1568-1579, Nov. 1999.

[4] E. Osalusi, J. Side, R. Harris, "Structure of turbulent flow in EMEC's tidal energy test site", *Internat. Comm. Heat and Mass Transfer*, vol 36, no. 5, pp. 422-431, May 2009.

[5] J. Thomson, B. Polagye, V. Durgesh, and M. C. Richmond, "Measurements of Turbulence at Two Tidal Energy Sites in Puget Sound, WA", *IEEE J. of Oceanic Eng.*, vol. 37, no. 3, pp 363-374, July 2012.

[6] J.-B. Richard, J. Bard, C. Rudolph, M. Milovich, "Assessing the capabilities of acoustic Doppler sensors for quantifying dynamic phenomena in tidal streams", in Proc. ICOE 2012.

[7] V. Nikora and D. Goring, "ADV Measurements of Turbulence: Can We Improve Their Interpretation?." J. Hydraul. Eng., vol 124, no. 6, pp 630–634, June 1998.

[8] *ADCP Coordinate Transformation, Formulas and Calculations*, Teledyne RD Instruments, 2010

[9] AWAC Acoustic Wave And Current Profiler, Nortek AS, 2010.

[10] V. Durgesh, J. Thomson, M. C. Richmond, B. L. Polagye, "Noise correction of turbulent spectra obtained from Acoustic Doppler Velocimeters", in review.

[11] B. H. Brumley, R. G. Cabrera, K. L. Deines, and E. A. Terray, "Performance of a Broad-Band Acoustic Doppler Current Profiler", *IEEE J. Oceanic Engineering*, vol. 16, no 4, pp. 402-407, Oct. 1991

[12] G. Voulgaris and J. H. Trowbridge, "Evaluation of the Acoustic Doppler Velocimeter (ADV) for Turbulence Measurements", *J. Atmos. Oceanic Technol.*, vol.15, no.1, pp. 272–289, Feb. 1998.

[13] M. C. Richmond, V. Durgesh, J. Thomson, and B. L. Polagye, "Inflow characterization for marine and hydrokinetic energy devices," Pacific Northwest Nat. Lab., Richland,WA, fy-2011: Annu. Progr. Rep., Tech. Rep. PNNL-20463, 2011.

[14] J.-B. Richard, J. Bard, J.-M. Rousset, B. Elsässer, K. Schröder, E. Robles Sestafe, M. Finn, and L. Johanning, "Update on Research activities in the MaRINET project", in Proc. EWTEC 2013.